Springer

KSME

Journal of Mechanical Science and Technology 31 (7) (2017) 3455~3464
www.springerlink.com/content/1738-494x(Print)/1976-3824(Online)
DOI 10.1007/s12206-017-0634-y

Development of numerical analysis model for resistance spot welding of automotive steel †

Yongki Lee, Hunchul Jeong, Kyungbae Park, Yougjun Kim and Jungho Cho*

School of Mechanical Engineering, Chungbuk National University, Cheongju 28644, Korea

(Manuscript Received November 30, 2016; Revised March 2, 2017; Accepted March 12, 2017)

Abstract

Resistance spot welding (RSW) is a process in which contacting metal surfaces are joined by the pressure and heat obtained from resistance to electric current flow. It is widely accepted in the industry due to its advantages in high speed and suitability for automation. The RSW process is extremely important to quality in automotive industry because approximately 6000 spot welds were used in automotive body. In addition, the RSW process is a complicated process that includes electrical, thermal and mechanical phenomena. For this reason, it is necessary that researchers should perform electric field, heat transfer and thermo-elastic-plastic analysis, and consider phase change, contact conditions and temperature dependence of material properties in order to simulate a realistic RSW process. There were lots of previous studies for RSW simulation by using Finite element method (FEM), but most of studies have performed qualitative analysis which predicts the shape of weld nugget fatigue life and residual stress. Therefore, this study defines the contents which mentioned above based on the theoretical background and reproduces a 3D DC RSW process through using ABAQUS, commercial FEM program. It also obtains the reliability in terms of simulation results through quantitative approach by comparing between the nugget shape and the actual experimental results. The error percentage of nugget width between simulation and experiment shows outstanding results that from 0.44 % to 3.80 %. Based on the simulation results through these theoretical backgrounds, it is possible to effectively trace the weld nugget shape of all steels, provided the temperature dependent material properties are available. An illustration of such a simulation to predict the nugget shape and size of resistance spot welded SPRC 340 steel is presented in the paper.

Keywords: Resistance spot welding; RSW; ABAQUS; Automotive steel; SPRC 340 steel; Weld nugget

1. Introduction

The RSW process is commonly used for welding thin plate, vehicle molar band, electronics and it is particularly significant in automotive industry because approximately 6000 spot welds were used in automotive body. During the RSW process, it fails to join if the heat input is not sufficient, on the contrary it leads to welding quality deterioration due to spatters caused by excessive heat. For these reasons, to find an optimal welding condition is significant according to the characteristic and quality of the weld materials. The quality evaluation after RSW process is primarily determined by the size of the weld nugget. There are lots of previous studies about RSW simulation by using the Finite element method (FEM) to predict the residual stress, fatigue life [1-5] and simulate the process of weld nugget formation. Kobayashi et al. simulate the 3D RSW process but which does not have the quantitative indicator and the simplified contact resistance, one of the significant variables, as a one value [6]. The RSW process simulation by using simplified value of contact resistance is also found in Refs. [7-11]. But simulating a process of weld nugget formation and predicting a weld nugget size are inappropriate if variables of contacting surfaces are not defined in detail. In addition, as most of these studies simulate by using 2D modeling [12-16], the application of 3D modeling is necessary considering the realistic RSW process, the multi-spot welding simulation and the scalability in many other shape of weld metals.

The main purpose of the simulation is to determine weld nugget size by comparing simulation to experiment. Governing equations are Maxwell's equation of conservation of charge and thermal energy balance equation.

2. Governing equations and background theory

In RSW, the generation of thermal energy which is required to melt the weld metal could be considered by joule heating. The joule heating arises when the energy dissipated by an electric current flowing through a process that a conductor is converted into thermal energy. Thermal-electrical coupling

*Corresponding author. Tel.: +82 43 261 2445, Fax.: +82 43 263 2441
E-mail address: junghocho@cbnu.ac.kr
† Recommended by Associate Editor Young Whan Park

arises from two sources. The conductivity in the electrical problem is temperature dependent, and the internal heat generated in the thermal problem is a function of electric current.

As aforementioned, it requires two governing equations to realize the virtual RSW process. The first one to introduce is Maxwell's equation of conservation of charge. Assuming steady-state direct current, the equation is expressed as

$$-\int_V \left(\nabla \delta\varphi\right)\cdot \boldsymbol{J} dV = \int_S \delta\varphi J dS + \int_V \delta\varphi r_c dV \tag{1}$$

where $J = -\boldsymbol{J}\cdot\boldsymbol{n}$ means the current density entering arbitrary control volume across the surface S.

The flow of electric current is described by Ohm's law and introducing this, the governing conservation of charge equation is expressed as

$$\int_V \left(\nabla\left(\delta\varphi\right)\sigma^E\right)\cdot\nabla\left(\varphi\right)dV = \int_V \delta\varphi r_c dV + \int_S \delta\varphi J dS\,. \tag{2}$$

Heat transfer process determined weld nugget shape in RSW. As the welding is performed in a short time due to the focused heat energy at the center of weld metal, heat condensed at the center and transferred to the periphery. The ellipsoid shape of the nugget is mainly due to the uneven ness in the heat loss from the nugget. The side adjacent to electrode would cool quickly then the other side as the heat absorption rate through electrode side is high due to the flow of coolant through electrode (an effective cooling system used to keep the temperature of electrode in check). The heat loss through radiation would be negligible compared to the heat absorbed by the electrode.

Physical situation has obviously suit the unsteady state, the boundary condition and etc. should be adjusted properly because the heat transfer analysis of RSW which used FEM occurs with transient heat transfer which varies the internal energy over the time. Through this transient heat transfer analysis, we can choose temperature distribution inside of the base metal, quantity of heat transfer and thermal stresses. In this study, heat conduction behavior is expressed as follows by Green and Naghdi's basic energy balance relation

$$\int_V \rho\dot{U}\delta\theta dV + \int_V \left(\nabla\left(\delta\theta\right)k\right)\cdot\nabla\left(\theta\right)dV$$
$$= \int_V \delta\theta r dV + \int_S \delta\theta q dS\,. \tag{3}$$

Eqs. (2) and (3) describe the electrical and thermal problems, respectively. As aforementioned, thermal-electrical coupling arises from two sources

Electrical problem
$$\sigma^E = \sigma^E\left(\theta\right). \tag{4}$$

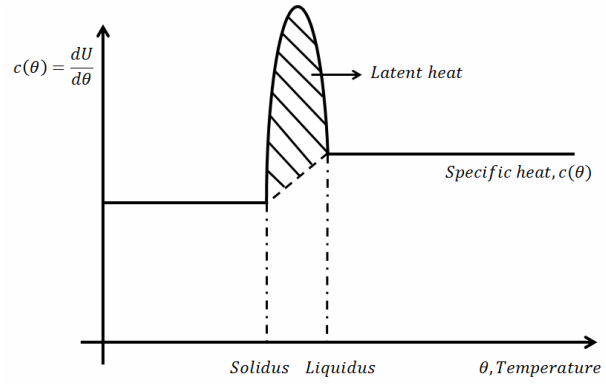

Fig. 1. The definition of latent heat.

Thermal problem
$$r = r_{ec}\left(\boldsymbol{J}\right) \tag{5}$$

where r is the heat generated within the base metal which is a function of electric current.

Joule's law describes the rate of electrical energy, P_{ec}, dissipated by current flowing through a conductor as

$$P_{ec} = \boldsymbol{E}\cdot\boldsymbol{J}\,. \tag{6}$$

In a transient analysis, an averaged value of P_{ec} is obtained over the increment. Thus the equation of P_{ec} can be expressed as

$$P_{ec} = \frac{1}{\Delta t}\int_{\Delta t} P_{ec}\,dt$$
$$= \left(\mathbf{E}\sigma^E\right)\cdot\boldsymbol{E} - \left(\boldsymbol{E}\sigma^E\right)\cdot\Delta\boldsymbol{E} + \frac{1}{3}\Delta\left(\boldsymbol{E}\sigma^E\right)\cdot\Delta\boldsymbol{E}\,. \tag{7}$$

The amount of this energy released as internal heat can be expressed as

$$r = \eta_c P_{ec}\,. \tag{8}$$

Constitutive equation for heat transfer problem is written about specific heat which commonly neglects the coupling between mechanical and thermal problem.

$$c\left(\theta\right) = \frac{dU}{d\theta}\,. \tag{9}$$

But the effect of latent heat in phase change is not satisfied above equation. Solidus temperature, liquidus temperature and the total internal energy which associated with the phase change are used in the phase change interval, respectively. When the latent heat is given, it is assumed to be in addition to the specific heat effect. Fig. 1 shows temperature dependant latent heat. The towering part in the middle of the figure plays a role to calculate energy dissipation in melting process.

$$\overline{c} = \rho c + \frac{L}{\theta_L - \theta_S}. \quad (10)$$

In addition, in case of carbon steel, specific heat value changes depending on carbon content, but specific heat value is commonly increasing sharply nearby 1003 K in most of carbon steel. Because the chemical change that converting the ferrite-pearlite to austenite has occurred. This phenomena generally causes the divergence problem of the simulation. Therefore, the application of the smooth curve is needed before and after 1003 K.

Generally, the stress analysis refers to the term which occurred by the power and gravity from the outside of the structure, but when it comes to the welding process analysis, it represents mainly the thermal stress which is generated by the sharp temperature change and non-uniformtemperature distribution. As coupled thermal-electrical analysis is progressed, it is possible to know the temperature distribution by the time change and then it makes to know the thermal strain. Accordingly, the thermal change according to the joule heating by electric current carries out the coupled thermal-electrical-structural analysis which makes the thermal stress analysis possible. In the coupled thermal analysis performing method, there are sequential coupled thermal analysis and fully coupled thermal analysis. Sequential coupled thermal analysis is the general access method that the structure analysis occurred by the result value after finishing heat transfer analysis. Completely coupled thermal analysis represents a method which occurs both the structure change and the thermal change simultaneously as time goes by. In this study, fully coupled thermal energy method is used and the analysis is conducted by adding about the part of electricity.

The metal follows the internal stress, strain from the elastic zone to the plastic zone according to the increase of load, external force. The yield point of the metal has usually the bigger point, it shows the plastic zone when it is under great external power. This characteristic is called as elastic-plastic. However, as the metal in the process of RSW process is accompanied by great temperature change, this makes the plastic deformation. This means that the properties of material are changed by temperature so deformation behavior is affected greatly by temperature. Thus, in order to predict the material deformation in RSW, thermo-elastic-plastic analysis should be conducted. This study applied thermal expansion coefficient, modulus of elasticity and yield strength by temperature to the model to figure out the thermo-elastic-plastic analysis.

3. Modeling and boundary conditions

Three dimensional analysis is conducted with five conditions from 5 kA to 9 kA by modeling the size of electrode and plate which are used in the actual RSW equally in order to simulate resistance spot welding process and compare and analyze with its actual result of the experimental. The analysis employed the commercial FEM program, ABAQUS 6.14

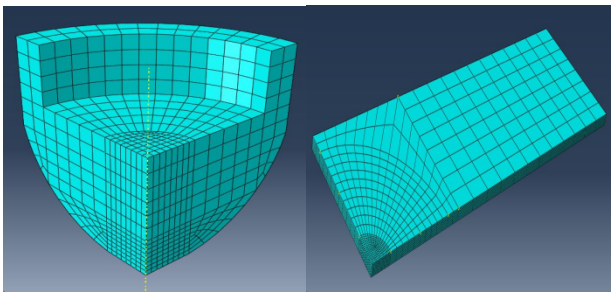

(a) Electrode (b) Plate

Fig. 2. Part modeling for RSW simulation.

and applied MKS system of unit. SPRC 340 steel and Chromium copper are used as the materials for the analysis model and they are modeling as shown in Fig. 2. It is noticeable that the contact center area is modeled with relatively fine meshes in circumference shape and the rest is with coarser in rectangular and this strategy finally made the simulation converge.

SPRC steel has thinner than hot rolled steel and has superior to it in the degree of accuracy. Also, its side is elegant, smooth, and superb in machinability. Due to the nature of it, it is utilized in automotive body, home appliances, furniture, architecture, and so on. Chromium copper is used mainly for the electrode of spot welding, projection welding, seam welding and also used for the secondary circuit structural member as it has high strength and conductivity. This property of the material appeared through chemical bond, heat treatment and cold working.

The weld metal is modeled by applying standard size of RSW specimen (100 mm*30 mm*1 mm), the electrode is modeled to dome shape of 6 mm in diameter, and the analysis is conducted after modeling for maintaining constant temperature during weld time by making water cooling channel at the top of the electrode. Mesh used hexahedron and Thermal-electrical-structural (Q3D8) element to conduct coupled thermal-electrical-structural analysis. Except for the case that the shape of weld metal is not a plate, the RSW model is mostly possible to design to the axially symmetrical model so modeling was completed to 1/4 size of the entire model when applying the axially symmetrical condition to cut down time the analysis time. Fig. 3 shows the model and the shape of mesh.

When the RSW analysis is conducted, the boundary conditions such as electrical, thermal, mechanical condition are used depending on the welding process parameter. Additionally, the physical phenomenon on the contact surface is considered. The electrical boundary condition which is used for the analysis employed the total 5 electric current condition from 5 kA to 9 kA by increasing per 1 kA in order to compare the actual result of the experimental under the same conditions and each condition as the current density input the data about the size of the upper electrode except for water cooling channel. In the lowest end of the electrode, the analysis is

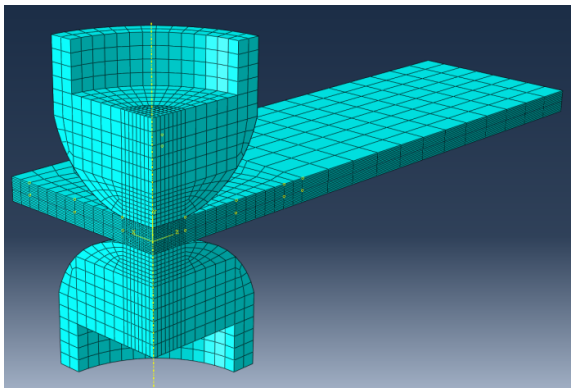

Fig. 3. Geometry of the assembled model and mesh.

conducted by giving the condition of 0 V to send an electric current to the whole model. The initial temperature of the RSW model and temperature of electrode water cooling channel are applied to 293 K and they are set up to be maintained constantly during a process of analyzing. The radiation condition meets the following formula and copies an ideal heat transfer by assuming as the black body that emissivity(ε) is 1.

$$q = A[(\theta)^4 - (\theta^0)^4]. \quad (11)$$

Here, A is a radiation constant and it means the value of multiplying emissivity by Stefan-Boltzmann constant. In case of the convective condition, the analysis is proceeded by giving natural convection condition to the following formula.

$$q = h(\theta - \theta^0). \quad (12)$$

Here h means convective heat transfer coefficient between the surface and θ^0 which is ambient sink temperature.

To simulate the electrode pressure, total force 300 kgf of the uppermost of the electrode is converted into Newton (N) unit and its value is put after dividing according to the axis-symmetry model. The lowest end and the uppermost of the electrode are bound not to be moved to the directions x, y, z, and the analysis is conducted by giving axis-symmetry condition to the directions x and y as the model of this study applied to the quarter of the size of the whole model.

There are two types of resistance in RSW. One is bulk resistivity, and the other is contact resistance between steel sheets. The contact resistance decreases nonlinearly as electrode pressing force increases. As the contacting interface is not totally flat, a lot of asperities remains either contacted or not when analyzing microscopically. Thus, the bigger the force applied is, the more asperities are. This means the increase of the real contact area so the contact resistance decreases. The whole resistance looks for the value by adding up bulk resistivity of the material and contact resistance. In other words, resistance value varies depending on bulk resistivity of the material, applied force, temperature. In this study, based on the definition by Greenwood and Babu et al., the contact resistance is obtained by considering bulk resistivity of material, force, and temperature and then the analysis is proceeded on the presumption that value of this graph is the whole resistance [17-19].

RSW is the welding method which welding is possible in a very short pace of time. Accordingly, in defining behavior of the contact surface, the analysis is conducted after assuming that there is no friction before the contact. Besides, normal behavior assumes that there is no stress before the contact and defines the condition that stress occurs after the contact. In coupled thermal-electrical analysis process, the heating occurs when the energy loss by the electric current which flows conductor is converted into thermal energy. In RSW process, the increase of temperature of plate is the largest proportion in the case by joule heating. Through this, the condition that the thermal energy by joule heating takes place was settled up in each contacting area.

As TCC (Thermal contact conductance) has different value on its result value according to surface roughness of the material in RSW, this can be represented to function about temperature and pressure like ECC (Electrical contact conductance). However, it is confirmed that the result of simulation according to the value of TCC is affected by the abnormal high value not the normal value of surface roughness through the simulation by Li et al. In other words, just one constant is entered by considering convergence of the analysis as the influence on the result of the simulation depending on temperature and pressure of TCC on the materials which are used normally is slight [20].

4. Welding process and material properties

There are four process of the whole process of RSW such as squeeze, weld, hold, off as mentioned above. The squeeze process can perform the stress analysis, the weld process can do the thermal stress and heat transfer analysis, and the subsequent processes can do residual stress and thermal strain analysis. This study does not include the part of stress and thermal strain but convers the squeeze cycle which perform the electrode force and the weld process which includes the exothermic reaction by the current to electrode force in order to predict the final weld nugget shape. For the welding conditions, electrode force 300 kgf, weld time 0.3 s, current from 5 ka to 9 ka which are mentioned above are employed and the analysis is carried out by measuring the amplitude like the following Fig. 4.

The weld metal, electrode and each material properties are entered to the graph which depends on temperature except for the density and the material properties considering the phase transformation with latent heat of weld metal was inputted. One of the parameters which is required to define bulk resistivity of weld metal, weld metal and yield strength of the electrode and ECC, the asperity density is measured approxi-

Table 1. Material properties of SPRC 340 steel at room temperature.

Property	Value
Density	7800 kg/m^3
Thermal conductivity	51.9 $W/m \cdot K$
Electric conductivity	8060000 $\mho/m$
Specific heat	450 $J/kg \cdot K$
Young's modulus	200 GPa
Poisson's ratio	0.27
Expansion coefficient α	0.00001 K^{-1}
Yield strength	245 MPa
Solidus temperature	1753 K
Liquidus temperature	1808 K
Latent heat	272000 J/kg

Table 2. Material properties of chromium copper at room temperature.

Property	Value
Density	8890 kg/m^3
Thermal conductivity	323 $W/m \cdot K$
Electric conductivity	44600000 $\mho/m$
Specific heat	385 $J/kg \cdot K$
Young's modulus	130 GPa
Poisson's ratio	0.30
Expansion coefficient α	0.0000176 K^{-1}
Yield strength	350 MPa

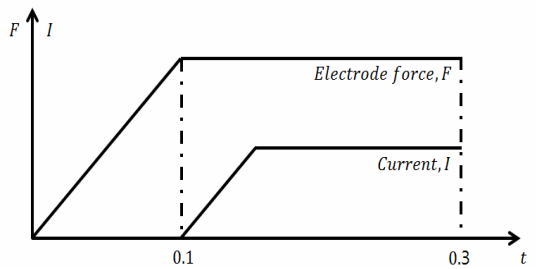

Fig. 4. The sequence of squeeze-welding cycle.

mately by using sigmoid function by Babu et al. The weld metal and the electrode material properties at room temperature are listed up in the following Tables 1 and 2.

5. Experiment and results

5.1 Temperature distribution

Performing the RSW experiment same with condition of analysis in order to compare the simulated results with the ABAQUS. Through surface polishing and etching, surface observation photograph of the weld zone has secured by cutting a cross-section after welding for macroscopic test. The

(a) Spot welder (b) Polisher

(c) Optical microscope (d) Diamond cutter

Fig. 5. Experimental apparatus.

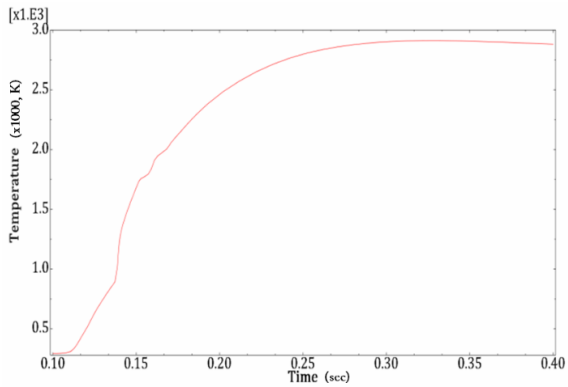

Fig. 6. Temperature changes in welding process.

etchant was composed of 6 % nital. Weld nugget size of the experimental results based on the measurement thickness of specimen that converted to pixels per unit length. Following Fig. 5 shows the experimental apparatus.

The temperature which rises rapidly above the melting temperature at plate-plate interface by current while the RSW progress and difference of the contact resistance in each interface. Temperature changes depending on time where the weld zone formed that is located in plate-plate interface are confirmed in following Fig. 6.

The weld nugget was formed in the around 0.06 s and confirmed that temperature at final step of the welding and the diameter of the weld nugget were proportional to current increasing. It also confirmed that the amount of indentation by

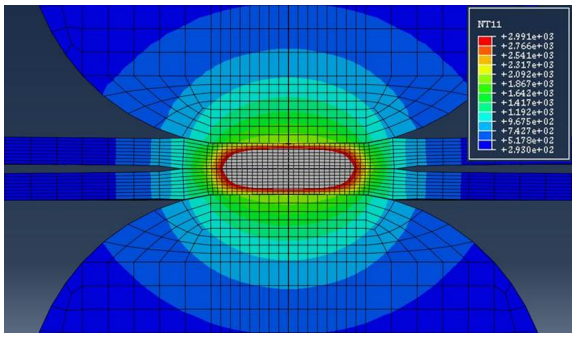

Fig. 7. Weld nugget formation at 0.3 s, 7 kA.

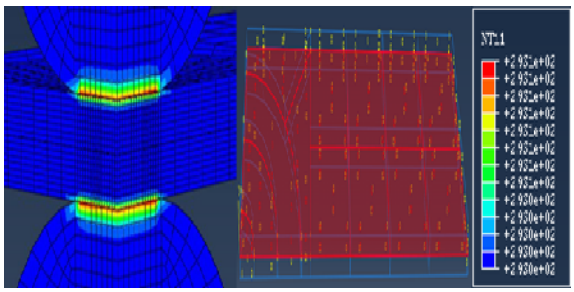

(a) Temperature distribution at initial step in the large contact area

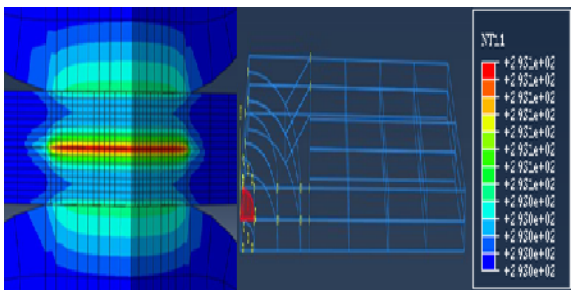

(b) Temperature distribution at initial step in the small contact area

Fig. 8. Comparison between large contact area and small contact area.

the electrode pressure and gap of the plate-plate interface near that place were increased gradually. Following Fig. 7 represents the weld nugget formation at 0.30 s in the current condition, 7 kA.

Theoretically, initial heat generation is generated in plate-plate interface because contact resistance of electrode-plate and plate-plate interface are different. This means contacting areas which plate-plate, upper electrode-plate and lower electrode-plate interface are same in model. However when overall contacting area set up equally, penetration has occurred considerably between electrode and periphery of the contacting area by the thermal deformation. We set up the contacting areas through overall plate area for preventing this phenomena, it cause the initial heat generation occurred in electrode-plate interface like Fig. 8.

The current has converged to the edge of the electrode as the surface was modeled to the shape of a dome which has the flat tale edge. For this reason, melting in the plate-plate interface started at periphery of the center. Finally the weld nugget

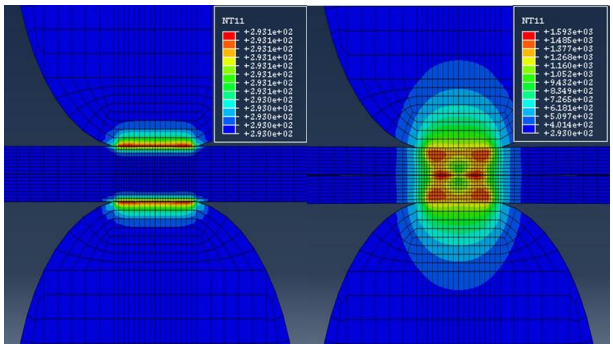

(a) Initial step (b) 0.05 s

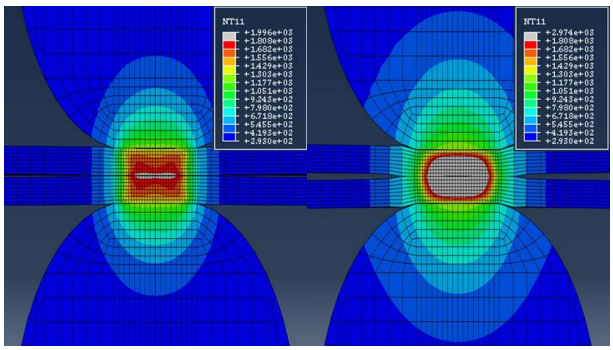

(c) 0.07 s (d) 0.30 s

Fig. 9. Temperature distribution during whole step along the time.

represents the lip shape because heat transfer is proceed to outward of weld zone and heat is gradually accumulated toward the center. Following Fig. 9 indicates the shape of the weld nugget by time change of analytical mode based on the 6 kA. Fig. 9(b) represents the formation process of the weld nugget by the concentration of current at edges of the electrode, and Fig. 9(c) represents the shape of weld nugget in a formative period.

5.2 Stress distribution

Figure shows the Von Mises stress distribution in squeeze cycle of RSW progress.

As shown in Fig. 10, the maximum stress has occurred at edge of the electrode, 139 MPa. Non-uniform stress distribution also occurred at contact area between electrode and weld metal which phenomena was reported a lot in other study [8, 9]. The reason for this phenomena is due to the electrode was not assumed rigid body but deformable body. If the electrode has assumed rigid body, the stress singularity which cause to divergence problem has occurred at the edge of the electrode.

Through addition of the generated thermal energy by current after the squeeze cycle, the thermal stress has occurred in weld cycle. In the center, weld nugget is formed by the thermal energy which occurred and compressive stress takes place by thermal expansion. On the contrary to this, tensile stress is given to the periphery part of the center which weld nugget is formed as heat occurs. This phenomenon can be confirmed

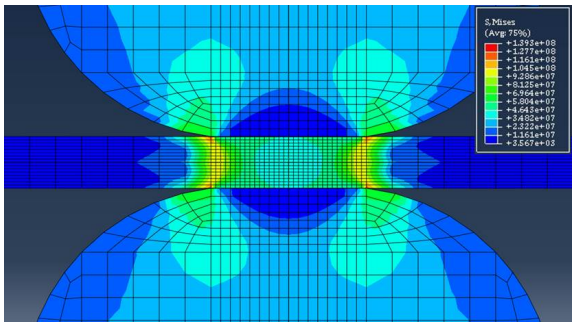

Fig. 10. Von Mises stress distribution at squeeze cycle.

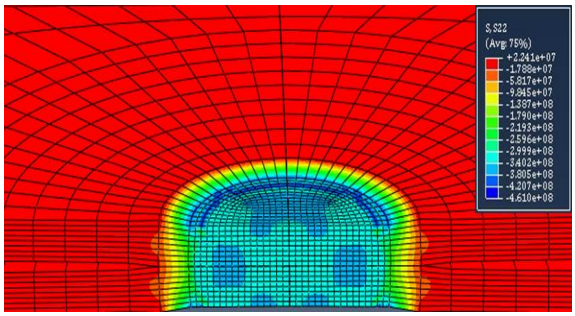

Fig. 11. Normal stress distribution at welding cycle.

by normal stress distribution. Normal stress in welding process at the final step (0.30 s) can be also confirmed as shown in Fig. 11. It shows the compressive stress has occurred in the center of weld zone and the tensile stress has occurred in the periphery of the center.

5.3 Plastic deformation

Plastic deformation is significant for the residual stress and thermal deformation but this study deals only with the physical meaning of the result of plastic deformation in welding process because residual stress and thermal deformation were not described. As weld nugget is formed, it and its periphery became under compression when welding is progressing and it leads to plastic deformation in the center because this phenomena generated in higher than yield point. Fig. 12 shows the plastic deformation at final step (0.30 s) of welding process and the greatest plastic deformation is occurred in edge of the contact area and formed the annular shape. This result serves to prevent the molten metal scattering to the outside during the welding process.

5.4 Comparison and analysis between experiment and simulation

The RSW experiment was performed under the same conditions to verify the reliability of the simulation results, which was compared and analyzed. However, as there are different criteria in each industry field, the result through a quantitative

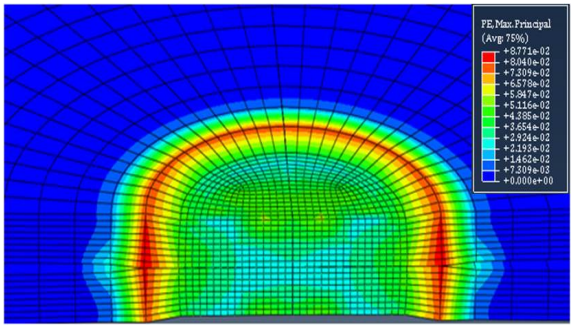

Fig. 12. Plastic strain distribution at 0.3 s.

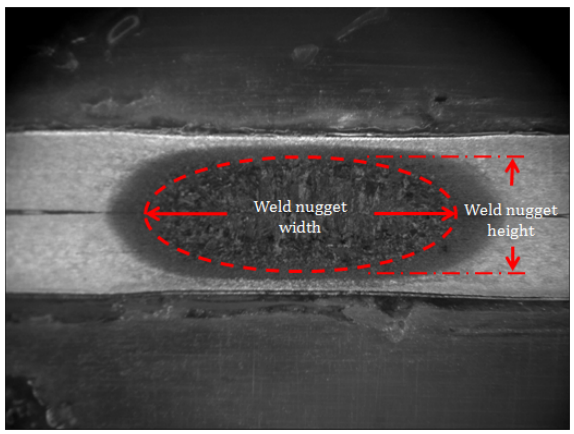

Fig. 13. Measurement a weld nugget size of experimental data.

approach of this study can be utilized as an indicator which meets each criteria efficiently in various fields.

Error factor about experimental data is obtained after measure the weld nugget diameter and height for comparison and analysis between simulation and experimental result. Size measurement method for the actual experimental results measure the thickness of the center of welded specimen at first and then measures each diameter and thickness in result photograph by converting it into the pixels per unit as shown in Fig. 13. Size measurement of simulation results was accomplished in analysis program. Comparison between simulation and experimental results are shown in Figs. 14-18. Digitized and obtained error factor compared to experiment are summarized in Table 3.

Previous studies which has the large deviation between experimental and simulation data. Also it has the large error factor in a singular condition which is over than 5 %. Compared to previous study, this study represent the error factor of weld nugget diameter about overall welding condition which against the experimental results from minimum 0.44 % to maximum 3.80 %. Weld nugget height in 5 kA and 6 kA, the results represent the highly error factor which are 18.25 % and 7.14 %, respectively. However, above the 7 kA condition, shows contented results that error factor within 3.29 %. The higher current creates thicker of weld nugget, but the phe-

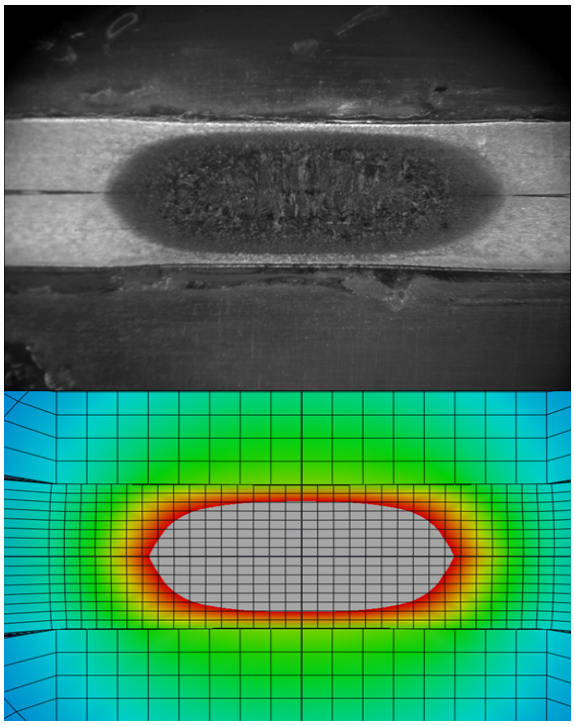

Fig. 14. Comparison between simulation and experiment, 5 kA.

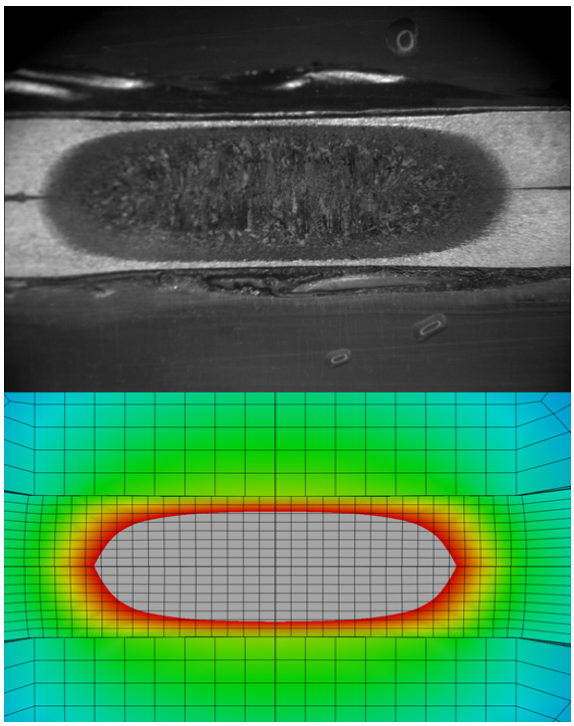

Fig. 15. Comparison between simulation and experiment, 6 kA.

nomenon that the result value drops is occurred again in 9 kA. It is considered by a phenomenon which is made by reducing the welding size itself as the higher current brings more indentation in the vertical direction in the part of the contact of specimen.

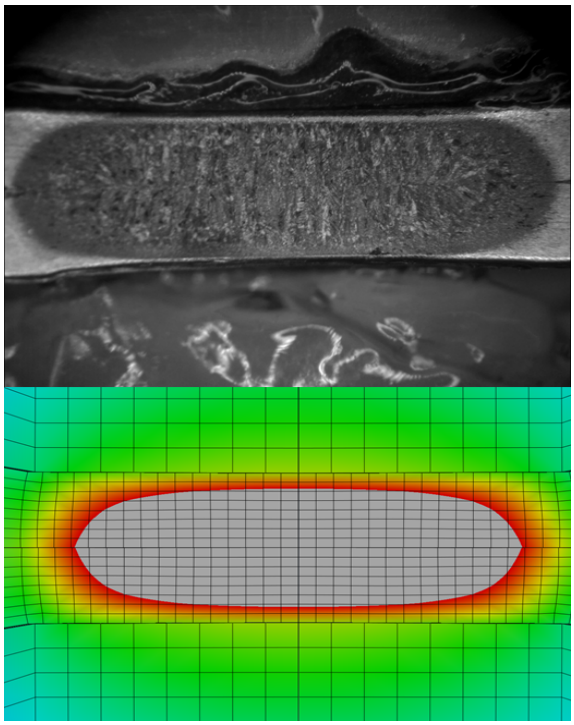

Fig. 16. Comparison between simulation and experiment, 7 kA.

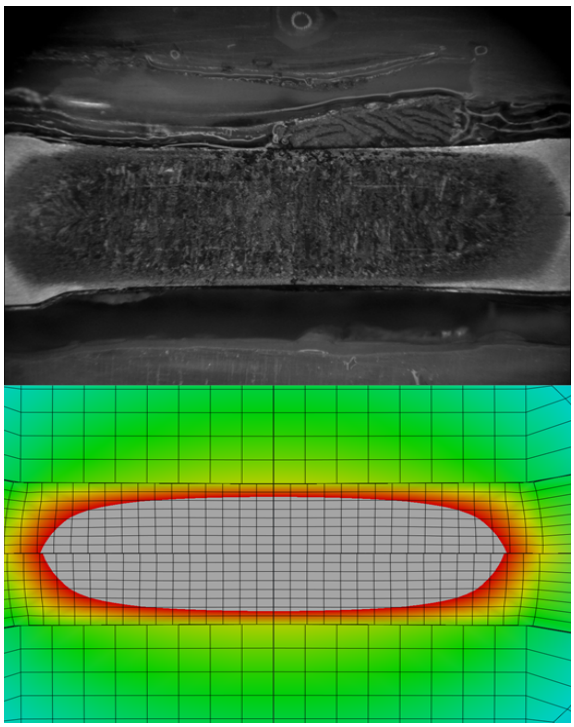

Fig. 17. Comparison between simulation and experiment, 8 kA.

6. Conclusion

In this study, by using commercial FEM program, ABAQUS about the DC RSW and simulate the RSW progress with 3d model for SPRC 340 steel. Stress analysis, heat con-

Table 3. Comparison nugget size between experiment and simulation.

No.	Center height (mm)	Nugget diameter (mm)		Nugget height (mm)		Mean absolute percent error of nugget diameter (%)	Mean absolute percent error of nugget height (%)
		Simulation	Experiment	Simulation	Experiment		
5 kA	1.84	3.72	3.75	1.49	1.26	0.53	18.25
6 kA	1.79	4.53	4.51	1.50	1.40	0.44	7.14
7 kA	1.70	5.14	5.26	1.51	1.48	2.09	2.2
8 kA	1.68	5.47	5.53	1.52	1.55	1.08	1.93
9 kA	1.63	6.27	6.04	1.47	1.53	3.80	3.28

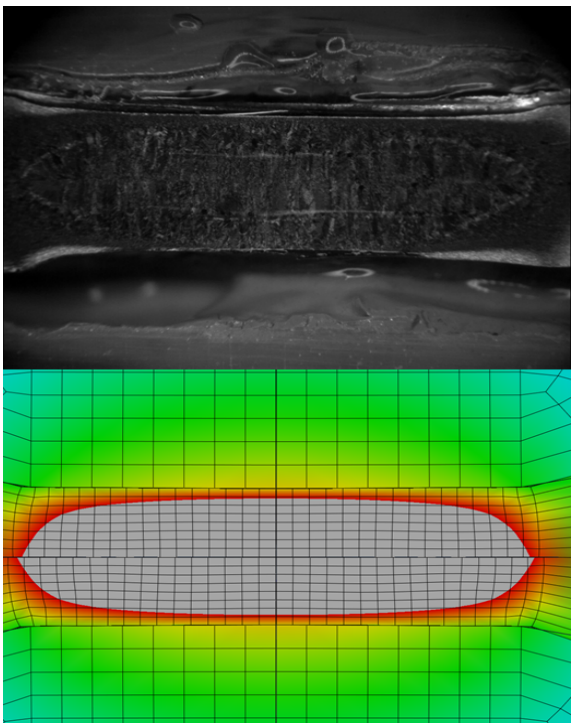

Fig. 18. Comparison between simulation and experiment, 9 kA.

duction analysis, electric field analysis and elastic-plastic analysis has conducted through the theoretical background by approaching qualitative analysis. Additionally, it secured the reliability of the analysis model through the quantitative analysis which comparison and analysis with experimental data for predicting the final weld nugget shape and size in RSW. To simulate the RSW progress, SPRC 340 steel and Chromium copper were used for this analysis model and results that error factor of weld nugget diameter shows from minimum 0.44 % to maximum 3.80 % compared to experimental results. It is expected to be accelerated through extensive study through the RSW simulation when temperature dependence material properties are secured for automotive steel.

Acknowledgement

This research was supported by Basic Science Research Program through the National Research Foundation of Korea (NRF) funded by the Ministry of Science, ICT and Future Planning, Korea (Grant No. 2016R1D1A1B03935036) and Technology Innovation Industrial Program funded by the Ministry of Trade, Industry & Energy, Korea (Grant No. 10052793).

Nomenclature

A : Radiation constant
c : Specific heat
E : Electric field intensity
h : Film coefficient
J : Current density entering the control volume
J : Current density
k : Thermal conductivity matrix
L : Latent heat of fusion
$\boldsymbol{n}$: Outward normal to control surface
P_{ec} : Rate of electrical energy
q : Heat flux per unit area
r : Heat generated within the body
r_{ec} : Internal volumetric current source
s : Second
S : Control surface
t : Thickness of bas metal
U : Internal energy
V : Control volume

Greek symbols

$\delta\varphi$: Electrical potential field
ε : Emissivity
η_c : Energy conversion factor
θ : Temperature
θ_L : Liquidus temperature
θ_S : Solidus temperature
θ^Z : Absolute zero on the temperature scale
θ^0 : Sink temperature
ρ : Density
σ^E : Electrical conductivity matrix
σ_{YS} : Density

References

[1] Y. Yang and J. Kim, Analysis of weldment by using finite

element method(3) - Residual stress and distortion in weldment, *Journal of The Korean Welding and Joining Society*, 29 (2011) 1-2.

[2] K. Kim, *Analysis and application of spot welding process by finite element method*, Chung Ang University (2000).

[3] Y. Yang, K. Son, S. Cho, S. Hong, S. Kim and K. Mo, Effect of residual stress on fatigue strength in resistance spot weldment, *Transactions of the Korean Society of Mechanical Engineers*, 25 (2001) 1713-1719.

[4] K. Kim, K. Jang and S. Kang, Finite element modeling for prediction of nugget shape and residual stress in resistance spot welding, *The Korean Welding and Joining Society Conference* (1999) 302-305.

[5] B. Joo, H. Byun and B. Lee, Performance evaluation for the methods of spot weld modeling considering durability, *Transactions of the Korean Society of Mechanical Engineers*, 29 (2005) 1153-1160.

[6] T. Kobayashi and Y. Mihara, Numerical simulation of nugget formation in spot welding, *SIMULIA Community Conference* (2014).

[7] H. Eisazadeh, M. Hamedi and A. Halvaee, New parametric study of nugget size in resistance spot welding process using finite element method, *Materials and Design*, 31 (2010) 149-157.

[8] H. A. Nied, The finite element modeling of the resistance spot welding process, *Welding Research Supplement* (1984) 123s-132s.

[9] C. L. Tsai, O. A. Jammal, J. C. Papritan and D. W. Dickinson, Modeling of resistance spot weld nugget growth, *Welding Research Supplement* (1992) 47s-54s.

[10] H. Zhigang, I.-S. Kim, W. Yuanxun, L. Chunzhi and C. Chuanyao, Finite element analysis for the mechanical features of resistance spot welding process, *Journal of Materials Processing Technology*, 185 (2007) 160-165.

[11] I. R. Nodeh, S. Serahzadeh and A. H. Kokabi, Simulation of welding residual stresses in resistance spot welding, FE modeling and X-ray verification, *Journal of Materials Processing Technology*, 205 (2008) 60-69.

[12] H. Zhigang, W. Yuanxun, L. Chunzhi and C. Chuanyao, A multi-coupled finite element analysis of resistance spot welding process, *Acta Mechanica Solida Sinica*, 19 (2006) 86-94.

[13] J. Saleem, A. Majid, K. Bertilsson, T. Carlberg and N. U. Islam, Nugget formation during resistance spot welding using finite element model, *International Science Index, Mechanical and Mechatronics Engineering*, 6 (2012) 1228-1233.

[14] Y. H. P. Manurung, N. Muhammad, E. Haruman, S. K. Abas, G. Tham, K. M. Salleh and C. Y. Chau, Investigation on weld nugget and HAZ development of resistance spot welding using SYSWELD's customized electrode meshing and experimental verification, *Asian Journal of Industrial Engineering*, 2 (2010) 63-71.

[15] O. Andersson, Process planning of resistance spot welding, *KTH Industrial Engineering and Management* (2013).

[16] C. Srikunwong, T. Dupuy and Y. Bienvenu, Numerical simulation of resistance spot welding process using FEA technique, *13th International Conference on Computer Technology in Welding* (2003).

[17] J. A. Greenwood, Construction resistance and the real area of contact, *British Journal of Applied Physics*, 17 (1966) 1621-1632.

[18] J. A. Greenwood and J. B. P. Williamson, Contact of nominally flat surfaces, *Proceedings of the Royal Society of London. Series A, Mathematical and Physical Sciences*, 295 (1966) 300-319.

[19] S. S. Babu, M. L. Santella, Z. Feng, B. W. Riemer and J. W. Cohron, Empirical model of effects of pressure and temperature on electrical contact resistance of metals, *Science and Technology of Welding and Joining*, 6 (3) (2001) 126-132.

[20] Y. B. Li, X. M. Lai and G. L. Chen, The influence of interfacial thermal contact conductance on resistance spot weld nugget formation, *Advanced Materials Research*, 97-101 (2010) 3239-3242.

Jungho Cho received his Ph.D. at KAIST in 2007 and now he is a faculty of Chungbuk National University after working at Hyundai Motors and Ohio State University, USA for several years. His major is development of welding and joining techniques, welding physics and thermo-dynamical analysis of weld pool.